AMOUR - Generalized Multi-Carrier Transceivers for Blind CDMA Regardless of Multipath*

Georgios B. Giannakis[1], Zhengdao Wang[1], Anna Scaglione[1], Sergio Barbarossa[2]

Abstract—**Suppression of multiuser interference (MUI) and mitigation of multipath effects constitute major challenges in the design of third-generation wireless mobile systems. Most wideband and multicarrier uplink CDMA schemes suppress MUI statistically in the presence of unknown multipath. For fading resistance, they all rely on transmit- or receive-diversity and multichannel equalization based on bandwidth-consuming training sequences, or, self-recovering techniques at the receiver end. Either way, they impose restrictive and difficult to check conditions on the FIR channel nulls. Relying on block-symbol spreading, we design A Mutually-Orthogonal Usercode-Receiver (AMOUR) system for quasi-synchronous (QS) blind CDMA that eliminates MUI deterministically and mitigates fading regardless of the unknown multipath and the adopted signal constellation. AMOUR converts a multiuser CDMA system into parallel single-user systems regardless of multipath and guarantees identifiability of users' symbols without restrictive conditions on channel nulls in both blind and non-blind setups. An alternative AMOUR design called Vandermonde Lagrange (VL) AMOUR is derived to add flexibility in the code assignment procedure. Analytic evaluation and preliminary simulations reveal the generality, flexibility, and superior performance of AMOUR over competing alternatives.**

Keywords— **Multi-Carrier CDMA, multipath fading channels, blind equalization, multiple rates**

I. Introduction

Multiuser interference (MUI) and multipath-induced intersymbol/interchip interference (ISI/ICI) are critical performance limiting factors in the design of third-generation wireless systems because they define their capabilities in handling high data rates and interactive multimedia services. MUI and ICI suppression is thus of paramount importance in mobile wideband CDMA standards such as UMTS and IMT-2000 [14]. Multipath causes frequency-selective fading, destroys orthogonality of user codes, and when unknown, it precludes usage of linear zero-forcing (ZF), minimum mean-square error (MMSE) [28], or nonlinear (decision-feedback (DF) and maximum-likelihood) multiuser detectors for MUI suppression [28]. But even when multipath channel estimates are available (e.g., using bandwidth-consuming training sequences) it is known that especially for multichannel uplink CDMA systems multiuser equalization is only possible under certain rank conditions on channel matrices that are difficult to check at the receiver [5, 23].

Thanks to their versatility in handling variable rates, relaxed requirements for power control, and minimal co-operation among users, self recovering (blind) CDMA receivers are appealing for mobile radio and digital broadcasting systems. However, even for the constrained class of equalizable channels blind receivers require subspace decompositions (see e.g., [1, 12, 24]), or, they suppress MUI statistically (and thus asymptotically) when reduced complexity adaptive receivers are sought [23, 26]. Antenna diversity trades off improved performance for receiver complexity and statistical MUI suppression [5]. Generalizing Orthogonal Frequency-Division Multiple Access (OFDMA), the recent, so called Lagrange - Vandermonde (LV) CDMA transceivers [18], have low complexity and offer blind MUI elimination. But similar to OFDMA and depending on the multipath channel, LV transceivers require extra diversity to ameliorate (but not eliminate) fading effects caused by channel nulls [17]. User code hopping and maximal ratio combining diversities have also been employed to combat fading in the increasingly popular (albeit bandwidth expanding) multicarrier (MC) CDMA [2, 4, 21]. Performance of MC DS-CDMA systems was evaluated over a frequency selective Rayleigh channel and compared with that of a single-carrier RAKE system in [11].

In the downlink, where all users share one common multipath channel, it has been shown that appropriately designed precoding guarantees identifiability of the users' symbols regardless of the underlying channel [19]. Various (non-)blind equalizers have also been derived in [19] and [20] (see also [29] and [27] for fractionally spaced detectors). In the uplink however, no existing system guarantees complete MUI cancellation and identifiability of the users' symbols without restrictions on the multipath channels involved.

Relying on block-symbol spreading, we develop in this paper A Mutually-Orthogonal User code-Receiver (AMOUR) structure for quasi-synchronous (QS) blind *uplink* CDMA that eliminates MUI deterministically and mitigates fading regardless of the (possibly unknown) multipath. In QS-CDMA systems, mobile users attempt to synchronize with the base-station's pilot waveform (see e.g., [3, 9]). But exact synchronization is difficult to implement due to multipath and Doppler effects arising because of relative motion, especially when the chip period is small.

The system designed here encompasses LV-CDMA and MC-CDMA systems as special cases, can have low FFT-based complexity, and offers considerable design flexibility. Although our design targets the uplink CDMA channel, it can be also applied to the downlink channel as well as to other wire-line applications such as DSL (Digital Subscriber Lines). Our focus will be on the blind scenario but AMOUR is also attractive when the multipath channel has been estimated (e.g., via pilot signals). Based on the filterbank block model of Section II, we develop the AMOUR-CDMA system in Section III and show that our design con-

[1]G. B. Giannakis, Z. Wang and A. Scaglione are with the Dept. of Electrical and Computer Engr., Univ. of Minnesota, 200 Union Street SE, Minneapolis, MN 55455. Tel/fax: (612)626-7781/625-4583; Email: {georgios,zhengdao,anna}@ece.umn.edu

[2]S. Barbarossa is with the Infocom Dept., Univ. of Rome "La Sapienza", Roma; ITALY. (sergio@infocom.ing.uniroma1.it)
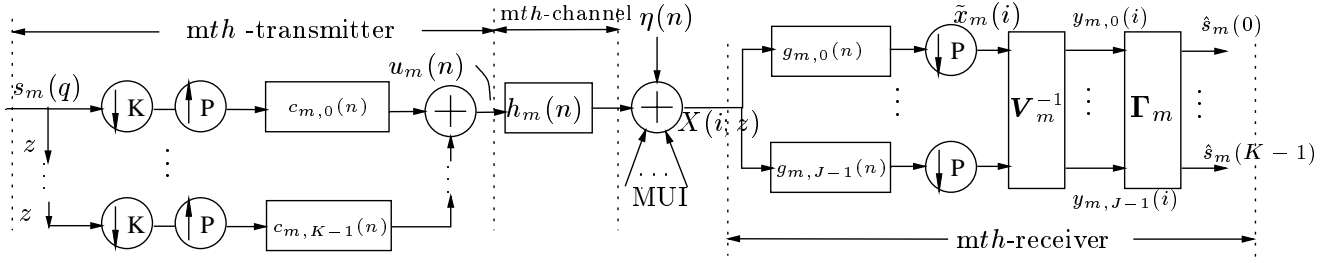
Fig. 1. Discrete-time baseband (VL-)AMOUR system

verts the multiple-input multiple-output (MIMO) CDMA to a set of parallel single-input single-output (SISO) systems. In Section IV we design a low complexity system and illustrate the basic idea of AMOUR with a simple example. Section V presents an alternative AMOUR system that adds flexibility in the code assignment procedure. Section VI deals with blind equalizer design and Section VII is devoted to performance analysis and comparisons with competing schemes via simulations.

II. AMOUR SYSTEM MODELING

A discrete-time baseband filterbank CDMA model was introduced in [24, 25], where the continuous CDMA spreading waveform was modeled as a chip-rate sampled code sequence followed by chip-rate pulse-shape filtering. Generalizing the CDMA model of [24, 25], the block diagram in Fig. 1 represents the discrete-time equivalent *baseband* model of our CDMA uplink system (transmitter and receiver filters for only one, the mth, user are shown). Advance elements (z) and downsamplers by K parse the mth user's information symbol stream $s_m(q)$ into consecutive blocks of length K. Upsamplers by P insert $P-1$ zeros between successive symbols and thereby convert symbol rate to chip rate[1]. Specifically, the kth downsampler's output is $s_m(qK + k)$, while the corresponding upsampler's output is $s_m(qK/P + k)\delta(q \bmod P)$, where δ stands for Kronecker's delta. Spreading of the kth symbol in each block is performed with a P-long FIR filter having as impulse response the code $c_{m,k}(n)$ and producing at its output the sequence: $s_m(\lfloor qK/P \rfloor + k)c_{m,k}(q \bmod P)$, where $\lfloor \ \rfloor$ denotes the integer floor. With $q = iP + p$, the kth filter output can be re-written as: $s_m(iK + k)c_{m,k}(p)$, where $p \in [0, P-1]$ and $k \in [0, K-1]$. The transmitted sequence $u_m(n)$ is the superposition of all chip sequences from the K branches of the filterbank, and with chip index $n = iP + p, p \in [0, P-1]$, it can be expressed as:

$$u_m(i;p) := u_m(iP + p) = \sum_{k=0}^{K-1} s_m(iK + k)c_{m,k}(p) . \quad (1)$$

In a nutshell, each of the M users spreads successive K-long symbol-blocks $\boldsymbol{s}_m(i) := [s_m(iK), \ldots, s_m(iK + K - 1)]^T$ to P-long chip-blocks $\boldsymbol{u}_m(i) := [u_m(iP), \ldots, u_m(iP+P-1)]^T$ (^{T} denotes transpose and K, P are design parameters to be specified in Section III). The chip sequence $u_m(n)$ is then transmitted at a rate $1/T_c$ after being D/A (digital-to-analog) converted

[1] Throughout this paper, we will use q (respectively n) for symbol- (chip-) time index; i for both symbol- and chip-block index, and k (respectively p) for symbol (chip) index within the ith block. Boldface (lower) upper case symbols will be used for (column vectors) matrices.
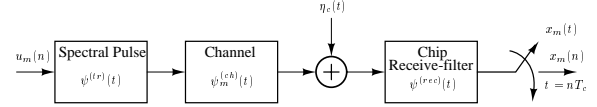
(not shown in Fig. 1) and filtered by the spectral-shaping pulse $\psi^{(tr)}(t)$ as depicted in Fig. 2.

Fig. 2. Continuous-time channel at chip rate

The transmitted signal $u_m(t)$ propagates through a (perhaps unknown) dispersive channel represented by its complex envelope $\psi_m^{(ch)}(t)$ and through the receive filter $\psi^{(rec)}(t)$. We define $h_m(t)$ to be the overall impulse response of the continuous-time channel including the transmitter and receiver filters; i.e., with $\star$ denoting convolution, $h_m(t) := \psi^{(tr)}(t) \star \psi_m^{(ch)}(t) \star \psi^{(rec)}(t)$. The received baseband signal from user m is thus given by $x_m(t) = \sum_{n=-\infty}^{\infty} u_m(n)h_m(t - nT_c - \tau_m)$, where τ_m is the propagation delay. The received signal from all users is therefore $x(t) = \sum_{m=0}^{M-1} x_m(t) + \eta_c(t) \star \psi^{(rec)}(t)$, If the received signal is sampled at the chip rate (every T_c seconds), then the discrete-time received sequence is: $x(n) := x(t)|_{t=nT_c} = \sum_{m=0}^{M-1} x_m(n) + \eta(n) = \sum_{m=0}^{M-1} \sum_{l=0}^{L_m} h_m(l)u_m(n-l) + \eta(n)$, where: $x_m(n) := x_m(t)|_{t=nT_c}$, $h_m(l)$ is the L_mth-order chip-rate sampled version of the continuous-time impulse response: $h_m(l) := h_m(lT_c - \tau_m)$, and similarly $\eta(n) := [\eta_c(t) \star \psi^{(rec)}(t)]|_{t=nT_c}$. Substituting $n = iP + p$, we can express the received chip sequence $x(i;p) := x(iP + p)$ as:

$$x(i;p) = \sum_{m=0}^{M-1} \sum_{l=0}^{L_m} h_m(l)u_m(iP + p - l) + \eta(iP + p) . \quad (2)$$

As we mentioned in the introduction, the downlink scenario is a special case of our setup and corresponds to having $h_m(l) = h(l), \forall m \in [0, M-1]$. In addition to $\bar{L}_m$ taps (corresponding to transmit-receive filter taps and chip-sampled paths), $h_m(l)$ in (2) includes the mth user's asynchronism d_m in the form of delay factors; i.e., its transfer function is given by: $H_m(z) = \sum_{l=0}^{L_m} h_m(l)z^{-l} = z^{-d_m} \sum_{l=0}^{\bar{L}_m} h_m(l + d_m)z^{-l}$. We suppose our block transmissions to be quasi-synchronous (QS) which amounts to having $d_m \ll P$. If $u_m(iP + p - l) = 0$ for $(p - l) \in [-L_m, 0]$ in (2), then the ith received block $\boldsymbol{x}(i) := [x(iP) \cdots x(iP + P - 1)]^T$ depends only on the ith transmitted blocks $\{\boldsymbol{u}_m(i)\}_{m=0}^{M-1}$; otherwise, the channels $h_m(l)$ introduce interblock interference (IBI). To enable QS transmissions and IBI-free receptions we assume that:

as1) *the FIR channels have maximum order $L := \max_m L_m = \bar{L} + D$ which incorporates the maximum number of chip-sampled*

taps $\bar{L}$ and the maximum delay $D := \max_m d_m \ll P$. To avoid IBI, we take $P > L$ and zero-pad our P-long codes $c_{m,k}(n)$ with L trailing zeros; i.e., $c_{m,k}(n) = 0$ for $n \notin [0, P - L - 1]$. Zero-padding our codes equips our block transmissions in (1) with L trailing zeros (guard chips); hence, all the terms $u_m(iP + p - l)$ in (2) belong to the ith block $\boldsymbol{u}_m(i)$ which can thus be written as $u_m(i; p - l)$ confirming elimination of IBI. Similar to OFDM, IBI removal can also be achieved by using a cyclic prefix instead of the L trailing zeros. Being affected by IBI, the cyclic prefix must of course be discarded at the receiver (we will explore such alternatives in Section V).

In Fig. 1, the ith received IBI-free block $\boldsymbol{x}(i)$ consists of chips from the mth user of interest along with MUI chips from other users and AGN $\boldsymbol{\eta}(i) := [\eta(iP) \cdots \eta(iP + P - 1)]^T$. We will find it convenient to cast our system's input-output relationship in the $\mathcal{Z}$-domain. Towards this objective, we define the $\mathcal{Z}$-transforms $C_{m,k}(z) := \sum_{n=0}^{P-1} c_{m,k}(n)z^{-n}$, $X(i; z) := \sum_{p=0}^{P-1} x(iP+p)z^{-p}$, $N(i; z) := \sum_{p=0}^{P-1} \eta(iP+p)z^{-p}$, and the $P \times 1$ Vandermonde vector $\boldsymbol{v}_P(\rho)$ built from the complex constant ρ as: $\boldsymbol{v}_P(\rho) := [1, \rho^{-1}, \ldots, \rho^{-(P-1)}]^T$. With z replacing ρ, the Vandermonde vector $\boldsymbol{v}_P(z)$ describes the $\mathcal{Z}$-transform operation in the sense that $X(i; z) = \boldsymbol{v}_P^T(z)\boldsymbol{x}(i)$. Since our P-long blocks are IBI-free, despite the presence of MUI and ISI/ICI that is allowed in our QS setup, one can focus on each received block separately. Substituting (1) into (2) and $\mathcal{Z}$-transforming with respect to p we can express the ith received block in the $\mathcal{Z}$-domain as:

$$X(i; z) = \sum_{\mu=0}^{M-1} H_\mu(z) \sum_{k=0}^{K-1} s_\mu(iK + k)C_{\mu,k}(z) + N(i; z). \quad (3)$$

Proceeding with our block diagram in Fig. 1 and with J denoting a design parameter (to be specified later), the receive-filterbank consists of J parallel filters (each of length P) that we describe by the $J \times P$ matrix $\boldsymbol{G}_m$ whose (j, p)th entry is $g_{m,j}(P - 1 - p)$. The columns of $\boldsymbol{G}_m$ (the pth denoted by $[g_{m,0}(P - 1 - p) \cdots g_{m,J-1}(P - 1 - p)]^T$) perform block filtering of $\boldsymbol{x}(i)$. Through $\boldsymbol{G}_m$, the block $\boldsymbol{x}(i)$ is mapped to a transformed ($\mathcal{Z}$) domain where user m is separated from its MUI. Downsamplers by P bring the transformed MUI-free block back to the symbol rate block $\tilde{\boldsymbol{x}}(i)$.

After MUI elimination performed by the $\boldsymbol{G}_m$ matrix in the $\mathcal{Z}$-domain, the $J \times J$ matrix $\mathbf{V}_m^{-1}$ performs the inverse transform on $\tilde{\boldsymbol{x}}(i)$, to yield the $J \times 1$ vector $\boldsymbol{y}_m(i) := [y_{m,0}(i) \cdots y_{m,J-1}(i)]^T$. Finally, block symbol estimates $\hat{\boldsymbol{s}}_m(i)$ are obtained by multiplying $\boldsymbol{y}_m(i)$ with the equalizer $\boldsymbol{\Gamma}_m$ (matrices $\boldsymbol{G}_m$, $\mathbf{V}_m^{-1}$, and $\boldsymbol{\Gamma}_m$ will be specified in Section III).

Our goal is to design code polynomials $\{C_{m,k}(z)\}_{m,k=0,0}^{M-1,K-1}$ and receive-filters $\{G_{m,j}(z)\}_{j=0}^{J-1}$, where $G_{m,j}(z) := \sum_{n=0}^{P-1} g_{m,j}(n)z^{-n}$, that guarantee: i) deterministic MUI cancellation with a simple linear receiver; ii) blind channel equalization; and iii) symbol recovery regardless of the channels, the adopted signal constellation and with minimum transmit-redundancy (and hence maximum bandwidth efficiency).

III. MUI/ISI-RESILIENT TRANSCEIVER DESIGN

We target MUI elimination in the frequency ($\mathcal{Z}$-) domain based on the received data model (3). A simple observation from

(3) is that the time-domain FIR convolutive channels $h_\mu(n)$ become multiplicative in the frequency ($\mathcal{Z}$-) domain. Therefore, if the users send their information via different frequencies (or subcarriers), they can be separated because frequency-domain orthogonality among transmissions is preserved at the receiver regardless of the multipath channels. OFDMA offers such a possibility too, because each user sends one symbol at a time using one frequency (see e.g., [16]). But if a channel's transfer function has a zero on (or close to) an information-bearing frequency, the corresponding user's symbol will be nullified. Therefore, OFDMA can not guarantee symbol recovery and necessitates frequency hopping to mitigate frequency-selective fading [16].

To enable symbol recovery in the presence of ISI, one may adopt a multi-carrier approach and have every information symbol ride over more than one frequencies [11]. Since the channels are assumed to have $\leq L$ zeros, if the same symbol is sent on more than L subcarriers, at least one subcarrier will survive the channel nulls – an approach reminiscent of repetition coding that guarantees symbol recovery at the expense of an L-fold bandwidth expansion. Convolutional coding has also been considered to improve BER performance [15], but bandwidth is still over expanded. Our approach to assuring symbol recovery while retaining high bandwidth efficiency, is to have each AMOUR user transmit a block of K (≥ 1) symbols simultaneously on $J \geq L + K$ user-specific subcarriers. After MUI is eliminated in the frequency-domain, judicious spreading enables recovery of K symbols from *any* $J - L$ of the J subcarrier signals.

We will consider general "subcarrier frequencies" on the $\mathcal{Z}$-plane rather than those on the unit circle only (one reason for terming our approach *generalized* MC-CDMA). With reference to (3), we will seek code polynomials $C_{m,k}(z)$, $m = 0, \ldots M-1$, so that for each m there exist J (a design parameter to be specified) different $\mathcal{Z}$-plane points $\{\rho_{m,j}\}_{j=0}^{J-1}$ on which $X(i; z)$ contains the mth user's contribution only but no MUI from the remaining $M - 1$ users, regardless of $\{H_\mu(z)\}_{\mu=0}^{M-1}$. Suppose for a moment that such MUI-free points $\rho_{m,j}$ exist and choose the mth receiver's filter as: $g_{m,j}(p) = \rho_{m,j}^{-(P-1-p)}$. The mth user's separating receiver filterbank assumes then a Vandermonde structure

$$\boldsymbol{G}_m = [\boldsymbol{v}_P(\rho_{m,0}) \cdots \boldsymbol{v}_P(\rho_{m,J-1})]^T . \quad (4)$$

Having points $\rho_{m,j}$ on which $X(i; z)$ is MUI-free by design, leads to a receiver output

$$\tilde{\boldsymbol{x}}_m(i) := \boldsymbol{G}_m\boldsymbol{x}(i) = [X(i; \rho_{m,0}) \cdots X(i; \rho_{m,J-1})]^T \quad (5)$$

that is also free of MUI. Note that the mth user-separating Vandermonde matrix $\boldsymbol{G}_m$ maps $\boldsymbol{x}(i)$ to preselected values of its $\mathcal{Z}$-transform $\tilde{\boldsymbol{x}}_m(i)$. We call these MUI-free points $\{\rho_{m,j}\}_{j=0}^{J-1}$ the *signature points* of user m, and henceforth we will denote with tilde $\mathcal{Z}$-domain quantities evaluated at those signature points.

A. MUI Eliminating Code and Receiver Design Principles

It follows from (3) that MUI elimination *regardless of multipath* is possible if and only if we design $\{C_{\mu,k}(z)\}_{\mu=0}^{M-1}$ such

that $\forall\, k \in [0, K-1]$, $j \in [0, J-1]$, it holds that:

$$C_{\mu,k}(\rho_{m,j}) = \theta_m(j,k)\delta(\mu-m)\,, \quad \forall \mu,m \in [0, M-1]\,, \tag{6}$$

where $\theta_m(j,k)$ are arbitrary nonzero complex constants. Condition (6) implies that $\{\rho_{m,j}\}_{j=0}^{J-1}$ are roots common to all $C_{\mu,k}(z)$ except $C_{m,k}(z)$ — an observation that plays a key role in our MUI-free design. Plugging $z = \rho_{m,j}$ into (3), we obtain under (6)

$$X(i;\rho_{m,j}) = H_m(\rho_{m,j})s_m(iK+k)\theta_m(j,k) + N(i;\rho_{m,j})\,. \tag{7}$$

Substituting (7) into (5), we can then write $\tilde{\boldsymbol{x}}_m(i)$ free of MUI as:

$$\tilde{\boldsymbol{x}}_m(i) = \mathrm{diag}[H_m(\rho_{m,0})\ldots H_m(\rho_{m,J-1})]\boldsymbol{\Theta}_m \boldsymbol{s}_m(i) + \tilde{\boldsymbol{\eta}}_m(i), \tag{8}$$

where $\mathrm{diag}[H_m(\rho_{m,0})\ldots H_m(\rho_{m,J-1})]$ denotes a $J \times J$ diagonal matrix with diagonal entries $\{H_m(\rho_{m,j})\}_{j=0}^{J-1}$, $\boldsymbol{\Theta}_m$ is a $J \times K$ matrix with (j,k)th entry $\theta_m(j,k)$, and the noise term $\tilde{\boldsymbol{\eta}}_m(i) := [N(i;\rho_{m,0}),\ldots,N(i;\rho_{m,J-1})]^T$.

For fixed μ and k, (6) prescribes $C_{\mu,k}(z)$ at MJ points $\rho_{m,j}$. Thus, $C_{\mu,k}(z)$ polynomials that satisfy (6) in general should have degree $\deg[C_{\mu,k}(z)] \geq MJ-1$. The *minimum* degree polynomial with $\deg[C_{\mu,k}(z)] = MJ-1$ can be uniquely determined by Lagrange interpolation through the points $\rho_{m,j}$ as:

$$C_{\mu,k}(z) = \sum_{\lambda=0}^{J-1} \theta_\mu(\lambda,k) \prod_{\substack{m=0 \\ (m,j)\neq(\mu,\lambda)}}^{M-1} \prod_{j=0}^{J-1} \frac{1-\rho_{m,j}z^{-1}}{1-\rho_{m,j}\rho_{\mu,\lambda}^{-1}}\,. \tag{9}$$

Minimum degree code polynomial $C_{\mu,k}(z)$ means minimum length code $c_{\mu,k}(n)$, which in turn implies *minimum redundancy* transmissions for channel-transparent MUI elimination.

Recall now that the (j,p)th entry of $\boldsymbol{G}_m$ in (4) is $g_{m,j}(P-1-p) = \rho_{m,j}^{-p}$; hence, the receive-filter polynomials are:

$$G_{m,j}(z) = \sum_{p=0}^{P-1} \rho_{m,j}^{-(P-1-p)}z^{-p} = \frac{\rho_{m,j}^{-P+1} - \rho_{m,j}z^{-P}}{1-\rho_{m,j}z^{-1}}. \tag{10}$$

Interestingly, we can verify using (6) that the codes in (9) and the receiver-filters in (10), satisfy *for all* shifts $l \in [0, L]$ and $\forall m \neq \mu$, $\forall j,k$ the condition:

$$\begin{aligned}
[c_{\mu,k}(n-l) \star g_{m,j}(n)]\big|_{n=P-1} &= \sum_{p=0}^{P-1} c_{\mu,k}(p-l)\rho_{m,j}^{-p} \\
&= \rho_{m,j}^{-l}C_{\mu,k}(\rho_{m,j}) = 0\,.
\end{aligned} \tag{11}$$

Hence, we have been able to design A Mutually Orthogonal set of User-codes (9) and Receivers (10), which explains the AMOUR abbreviation of our design. We emphasize that (11) expresses orthogonality between receivers and shifted versions of the codes. From this viewpoint, (11) implies mutual orthogonality in the presence of all pure-delay channels $h_m(n) = \delta(n-l)$. Because any FIR channel is a linear combination of such elementary channels, codes and receivers satisfying (11) $\forall\, l \in [0, L]$ remain mutually orthogonal (and thus guarantee MUI-elimination) regardless of any Lth-order multipath channel.

B. Conditions on Block Spreading Codes for Symbol Recovery

Starting with MJ points on the complex plane, we have seen so far how to design MUI-resilient user codes and receivers. We consider next how to spread the K symbols by appropriately selecting the $\boldsymbol{\Theta}_m$ matrices so that symbol recovery can be guaranteed from $\tilde{\boldsymbol{x}}_m(i)$ in (8). Choosing $J \geq K$, we deduce from (8) that a necessary and sufficient condition to guarantee identifiability of symbols $\boldsymbol{s}_m(i)$ from $\tilde{\boldsymbol{x}}_m(i)$ with a linear receiver *regardless of* the input symbol *constellation* is:

$$\mathrm{rank}(\mathrm{diag}[H_m(\rho_{m,0})\ldots H_m(\rho_{m,J-1})]\boldsymbol{\Theta}_m) \geq K\,. \tag{12}$$

Constellation-independent linear receivers are attractive from a computational perspective and useful for initializing constant-modulus and decision-feedback (DF) alternatives. Unlike such nonlinear equalizers that require (at least partial) knowledge of the constellation, non-iterative linear receivers obviate error-propagation effects also.

Two possibilities of satisfying (12) arise:
• Case 1) if the mth transmitter has access to Channel State Information (CSI), namely $H_m(z)$, we can always choose $J = K$ different points $\rho_{m,j}$ so that $H_m(\rho_{m,j}) \neq 0\ \forall j \in [0, K-1]$; hence, with any non-singular $K \times K$ matrix $\boldsymbol{\Theta}_m$, we can fulfill (6) and (12).
• Case 2) if CSI is not available at the transmitters, since $H_m(z)$ has $\leq L$ roots, at most L of $\{H_m(\rho_{m,j})\}_{j=0}^{J-1}$ can be zero. Thus, in order to satisfy (12), we need: 2a) $J \geq L+K$; and 2b) any $J-L$ rows of $\boldsymbol{\Theta}_m$ to span the complex space of K-tuples $\mathbb{C}^K$.

In applications where channels are long, we may want to design our system with $J < L+K$ signature points which decreases the amount of spreading (MJ) and allows usage of smaller K's to reduce decoding delays. Suppose $L_b \leq L$ denotes the number of "bad signature points", i.e., those code polynomial roots that coincide with channel nulls. Symbol identifiability is then guaranteed when $L_b \leq \tilde{L} := J - K$. In fact, $\tilde{L}$ can be thought of as a diversity factor and as we illustrate in Section VII, considerable gains in Bit Error Rate (BER) are achieved with $\tilde{L}\ (< L)$ as small as 1 or 2 with Rayleigh fading channels. This feature makes the AMOUR system attractive in applications such as DSL and time-division duplex (TDD), where CSI is available at the transmitters. In such applications, we can even guarantee symbol recovery with $J = K$ as we discussed under Case 1.

Because our ultimate goal is channel-independent MUI elimination and blind symbol recovery, we focus subsequently on Case 2 and choose $J = L+K$, which will also turn out to achieve maximum bandwidth efficiency.[2] Formally stated, we design our transmitters to satisfy:
as2) $J = L+K$ and any K rows of $\boldsymbol{\Theta}_m$ are linearly independent.
One class of $\boldsymbol{\Theta}_m$'s satisfying as2) that will prove useful and flexible enough for our purposes is:

$$\boldsymbol{\Theta}_m = A_m[\boldsymbol{v}_K(\rho_{m,0})\cdots\boldsymbol{v}_K(\rho_{m,J-1})]^T, \tag{13}$$

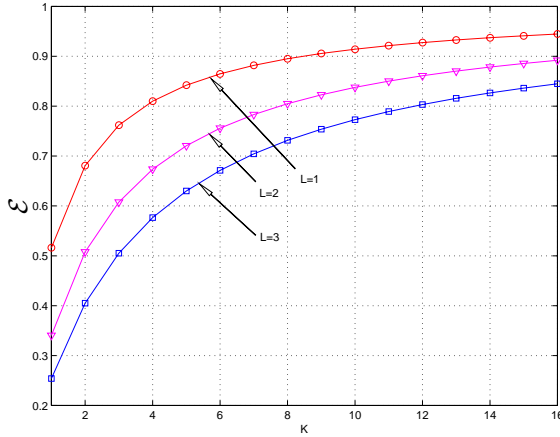[2]Larger J's however, may offer better resilience against frequency selective fading.

Fig. 3. Bandwidth efficiency for an AMOUR-CDMA system with 16 users

where A_m stands for the mth user's amplitude, and the points $\{\rho_{m,j}\}_{j=0}^{L+K-1}$ are distinct so that any K rows of the Vandermonde matrix $\boldsymbol{\Theta}_m$ in (13) are linearly independent. Defining $S_m(i;z) := \boldsymbol{v}_K^T(z)\boldsymbol{s}_m(i)$, one can recognize that when multiplied from the right by $\boldsymbol{s}_m(i)$, matrix $\boldsymbol{\Theta}_m$ in (13) evaluates $S_m(i;z)$ on the J signature points of user m; i.e.,

$$\boldsymbol{\Theta}_m \boldsymbol{s}_m(i) = A_m[S_m(i;\rho_{m,0})\ldots S_m(i;\rho_{m,J-1})]^T. \quad (14)$$

Based on (14), we will show in the next subsection that the MUI-free signal $\tilde{\boldsymbol{x}}_m(i)$ in (8) can be simplified nicely. But for now, let us look into AMOUR's bandwidth efficiency.

Taking into account the L trailing zeros, the code length in our system is [c.f. (9)]: $P = MJ + L = M(L+K) + L$, and since we deal with transmissions of K-long blocks from M users, the bandwidth efficiency of our system is

$$\mathcal{E} := \frac{MK}{P} = \frac{MK}{M(L+K)+L}. \quad (15)$$

For sufficiently large $K \gg L$, we have $\mathcal{E} \approx 100\%$; hence, bandwidth is not over expanded (see also Fig. 3). This unique feature of the AMOUR design is in sharp contrast with channel coding techniques that are employed together with interleaving to cope with errors induced by MUI and ISI (e.g., see [10], [15] and [30]). AMOUR block spreading codes are linear over the complex field while channel codes (designed over Galois fields) combat MUI and ISI at the price of increased complexity and bandwidth over expansion.

C. Back to the Time-domain — MIMO to SISO Equivalence

Having achieved user separation in (8), we show in this subsection how to recover $\boldsymbol{s}_m(i)$ from $\tilde{\boldsymbol{x}}_m(i)$ and how the AMOUR code selection of (13) converts the MIMO CDMA system to parallel user-specific SISO systems. Using (13) and (14), $\forall j \in [0, L+K-1]$, we can write (8) component-wise as

$$X(i;\rho_{m,j}) = A_m S_m(i;\rho_{m,j}) H_m(\rho_{m,j}) + N(i;\rho_{m,j}), \quad (16)$$

which confirms that we have achieved user separation at certain $\mathcal{Z}$-transform values of the ith received block. In the

noiseless case, (16) gives us J evaluations of the polynomial $S_m(i;z)H_m(z)$, which has maximum order $K+L = J$. From these evaluations, we can thus reconstruct $S_m(i;z)H_m(z)$ using Lagrange interpolation. To clarify how this can be achieved in the noisy case, let us consider the polynomial $Y_m(i;z)$ of maximum degree $J-1$ given by

$$Y_m(i;z) := A_m S_m(i;z)H_m(z) + N_m(i;z), \quad (17)$$

where $N_m(i;z)$ is the unique polynomial that satisfies: i) $\deg[N_m(i;z)] \leq J-1$; and ii) $N_m(i;\rho_{m,j}) = N(i;\rho_{m,j})$, $\forall j \in [0, J-1]$.

By comparing (16) with (17), one can readily see that $Y_m(i;\rho_{m,j}) = X(i;\rho_{m,j})$, $\forall j \in [0, J-1]$, or, in vector form: $\tilde{\boldsymbol{y}}_m(i) := [Y_m(i;\rho_{m,0}) \cdots Y_m(i;\rho_{m,J-1})]^T = \tilde{\boldsymbol{x}}_m(i)$. Let $\boldsymbol{y}_m(i) := [y_{m,0}(i) \cdots y_{m,J-1}(i)]^T$ denote the time-domain coefficient vector of $Y_m(i;z)$. Vector $\boldsymbol{y}_m(i)$ is related to $\tilde{\boldsymbol{y}}_m(i)$ through a $J \times J$ Vandermonde matrix $\mathbf{V}_m := [\boldsymbol{v}_J(\rho_{m,0})) \cdots \boldsymbol{v}_J(\rho_{m,J-1})]^T$; i.e., $\tilde{\boldsymbol{y}}_m(i) = \mathbf{V}_m \boldsymbol{y}_m(i)$. Matrix $\mathbf{V}_m$ is full rank because $\rho_{m,j}$'s were chosen to be distinct. It now follows that (recall also that $\tilde{\boldsymbol{x}}(i) := \boldsymbol{G}_m \boldsymbol{x}(i)$)

$$\boldsymbol{y}_m(i) = \mathbf{V}_m^{-1}\tilde{\boldsymbol{y}}_m(i) = \mathbf{V}_m^{-1}\tilde{\boldsymbol{x}}_m(i) = \mathbf{V}_m^{-1}\boldsymbol{G}_m \boldsymbol{x}(i), \quad (18)$$

which explains the role of the multivariate operation $\mathbf{V}_m^{-1}$ in the block diagram of Fig. 1. Indeed, matrix $\mathbf{V}_m^{-1}$ performs Lagrange interpolation and thus recovers the polynomial $Y_m(i;z)$ of order $J-1$ in (17) from its J evaluations offered by (16).

Note that (17) reveals another important feature of our AMOUR design: after applying the $\mathbf{V}_m^{-1}$ transformation, the multiuser CDMA (viewed as an MIMO system) is converted to M parallel single-user SISO systems regardless of the multipath (see also Fig. 4a).

In a time-domain vector form, (17) can also be written as (see also Fig. 4b):

$$\boldsymbol{y}_m(i) = A_m \mathbf{H}_m \boldsymbol{s}_m(i) + \boldsymbol{\eta}_m(i), \quad (19)$$

where $\boldsymbol{\eta}_m(i) := \mathbf{V}_m^{-1}\boldsymbol{G}_m \boldsymbol{\eta}(i)$ is the coefficient vector of the polynomial $N_m(i;z)$, and $\mathbf{H}_m$ is the Toeplitz convolution matrix built from the coefficients of $H_m(z)$ as:

$$\mathbf{H}_m := \begin{bmatrix} h_m(0) & \cdots & 0 \\ \vdots & \ddots & \vdots \\ h_m(K-1) & & h_m(0) \\ \vdots & \ddots & \vdots \\ 0 & \cdots & h_m(K-1) \end{bmatrix}_{(L+K) \times K}. \quad (20)$$

As long as the channel $h_m(n)$ has one non-zero tap, which is always true, $\mathbf{H}_m$ is full rank. This property will be exploited later on to construct single-user blind equalizers; e.g., the zero-forcing one: $\boldsymbol{\Gamma}_m^{(zf)} = \mathbf{H}_m^\dagger$, where $\dagger$ denotes matrix pseudo-inverse.

D. Links with MC-CDMA and LV-CDMA

In MC-CDMA, each symbol is spread with a user-specific code $\tilde{c}_m(l)$ having gain J, before being transmitted over J subcarriers that are shared by all the users. User separation at the receiver relies on the linear independence among user codes
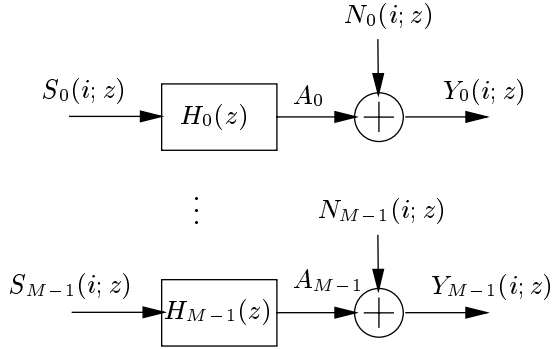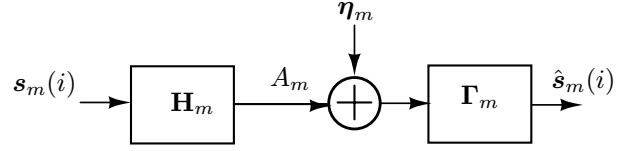
Fig. 4a. Equivalent parallel AMOUR-CDMA

Fig. 4b. Single user block (vector) model

[8]. With signature points on the unit circle, each AMOUR user transmits K (≥ 1) symbols using J subcarriers also, but subcarriers in AMOUR are user-specific. Our second reason for terming the AMOUR transceivers *generalized* multicarrier is that AMOUR subsumes MC-CDMA as a special case. To show this, we have to relax the mutual orthogonality condition (6), as transceivers in MC-CDMA are not mutually orthogonal in general. To establish the link, we must also choose $K = 1$ (no symbol blocking) and the signature points to be uniformly distributed around the unit circle as MC-CDMA subcarriers are common to all users: $\rho_{m,l} = \exp(j2\pi f_l)$, where $f_l = l/J$, $l \in [0, J-1]$. Under these conditions, MC-CDMA modulation with spreading gain J and code $\tilde{c}_m(l)$, can be implemented and viewed as a special AMOUR transmission with (Lagrange interpolating) code polynomials obeying the constraints:

$$C_m(\rho_{m,l}) = C_m(e^{j2\pi l/J}) = \tilde{c}_m(l)\,, \quad l \in [0, J-1]\,. \quad (21)$$

Note that the spreading codes in MC-CDMA manifest themselves as amplitude spectra of the AMOUR code polynomials $C_m(z)$. If $\tilde{c}_m(l)$ has constant modulus (e.g., if it is binary ±1), the corresponding AMOUR code spectrum will have equal magnitude at all J subcarriers. Such an even distribution of energy over the available bandwidth leads to reduced variation of the received SNR relative to that observed when DS-CDMA transmissions propagate through frequency-selective channels [7]. As we illustrate in our simulations, this competitive advantage of MC-CDMA over DS-CDMA is more pronounced in our general AMOUR design even for downlink transmissions (note that the special AMOUR codes in (21) corresponding to MC-CDMA do not satisfy (6)). Unlike AMOUR, MC-CDMA does not guarantee channel-independent demodulation in the uplink. Hopping and channel coding ameliorate performance degradation when deep fades are present but at the price of bandwidth expansion [2].

The AMOUR system also generalizes the LV/VL-CDMA systems of [17, 18], which also rely on symbol-periodic (as opposed to block) spreading and one signature point per user (as opposed to $L + K$ points used herein). LV/VL-CDMA also guarantees MUI elimination regardless of channel nulls. But when the channel nulls happen to coincide with one user's signature point, this user will suffer consistently. Even when one of the nulls is close to a user's signature point, BER performance will degrade considerably. Although our AMOUR design guarantees channel independent demodulation without resorting to

frequency hopping, signature point hopping along the lines of [2] can still be implemented to improve average performance further in the presence of frequency- and/or time-selective multipath (see also [17] and [18]). Signature point hopping and optimal selection of user signatures to enhance robustness of AMOUR against Doppler and frequency offset effects deserve further investigation and pertinent results will be reported elsewhere.

IV. Low Complexity AMOUR Design

In steps, AMOUR's general design procedure can be summarized as follows:
d1) Choose the symbol block length $K \gg L$;
d2) Select $MJ = M(L + K)$ distinct points $\rho_{m,j}$ on the complex plane and assign $J = L + K$ of them to be the signature points $\{\rho_{m,j}\}_{j=0}^{L+K-1}$ of the mth user;
d3) Compute the codes $c_{\mu,k}(n)$ according to (9) and add L trailing zeros as per as1);
d4) Set the receive-filters $g_{m,j}(p)$ according to (10) to isolate user m from its MUI;
d5) Compute as in (18) $\mathbf{V}_m^{-1}$ and design the equalization matrix $\mathbf{\Gamma}_m$ as will be discussed in Section VI.

A. Reduced Complexity Transceivers

Step d2) does not specify how to select $\rho_{m,j}$ on the complex plane. Selection of these signature points according to certain optimality criteria is an interesting research topic but will not be pursued here. However, we will look into specific choices for the signature points in (13) that lead to reduced-complexity designs.

Suppose $\rho_{m,j}$'s are chosen regularly around the unit circle. Specifically, with $l \in [0, L + K - 1]$ and using complex exponentials as signature points for user m, we select

$$\rho_{m,l} = e^{j\frac{2\pi(m+lM)}{M(L+K)}}\,, \quad m \in [0, M-1]\,. \quad (22)$$

User code polynomials with such signature points have coefficients given by (c.f. (9) and (13))

$$c_{m,k}(n) = \begin{cases} A_m e^{j\frac{2\pi m}{M}r}, & \text{if } n = r(L+K)+k, \\ 0, & \text{otherwise.} \end{cases} \quad (23)$$

Observe that for every user m, the code $c_{m,k}(n) = c_{m,0}(n-k)$ $\forall k = 0, \ldots, K-1$, which means that at the transmitter, the

spread chip sequence $u_m(n)$ in (1) is basically a convolution of $s_m(iK + k)$ with $c_{m,0}(n)$. But since $c_{m,0}(n)$ is non-zero only at multiples of $L + K$, this convolution entails a simple shift and scaling only. Hence, with codes as in (23) the transmitter in AMOUR has very low complexity. At the receiver, matrix inversion (of $\mathbf{V}_m$) and multiplications (by $\mathbf{V}_m^{-1}\boldsymbol{G}_m$) can be replaced by FFTs. Algorithmically, the receiver follows these steps:

r1) It computes a P-point FFT of the received block $\boldsymbol{x}(i)$ at the $M(L + K)$ frequencies given by (22) to obtain: $\tilde{\boldsymbol{y}}_m(i) = \tilde{\boldsymbol{x}}_m(i) = \boldsymbol{G}_m\boldsymbol{x}(i)$ for all $m = 0, 1, \ldots, M - 1$;

r2) For each of the M users, it performs an $(L+K)$-point IFFT at $L + K$ user-specific frequencies (signature points) to obtain: $\boldsymbol{y}_m(i) = \mathbf{V}_m^{-1}\tilde{\boldsymbol{y}}_m(i)$;

r3) For each user, it applies a (preferably linear) single user equalizer on $\boldsymbol{y}_m(i)$ to obtain $\hat{\boldsymbol{s}}_m(i) = \boldsymbol{\Gamma}_m\boldsymbol{y}_m(i)$.

The codes in (23) bring out a tradeoff that appears with AMOUR's selection of the block size K. On the one hand, one wants to have K as large as possible to reduce redundant overhead needed per block, or, equivalently to avoid bandwidth over expansion [c.f. (15)]. On the other hand, as K increases, the block gets longer and the decoding delay will increase proportionally. The channels are also required to remain time-invariant over a longer period. Furthermore, when one transmits more symbols per block, the peak-to-average power ratio will increase in general, and power amplifiers may have to increase their back-off values accordingly. From this *power-efficiency* viewpoint, the codes in (23) are particularly appealing because except for the guard intervals, they have constant modulus and thus lead to *constant modulus transmissions*.

Now, let us illustrate the basic idea of AMOUR design and its MUI eliminating ability with a simple example involving user codes as in (23).

B. A Design Example

Suppose $L = 1$ and $M = 3$. For simplicity, we choose $K = 2$ (recall that K should be much greater than L to avoid bandwidth over expansion). The signature points of the three users are shown in Fig. 5a equally spaced and interleaved along the unit circle; i.e., $\rho_{m,l} = \exp(j2\pi(m + 3l)/9)$, $m, l = 0, 1, 2$. Assuming $A_m = 1$, the user codes can be computed from (9) to be $C_{0,k}(z) = \frac{1}{3}(1+z^{-3}+z^{-6})z^{-k}$, $C_{1,k}(z) = \frac{1}{3}(1+e^{j\frac{2\pi}{3}}z^{-3}+e^{j\frac{4\pi}{3}}z^{-6})z^{-k}$, $C_{2,k}(z) = \frac{1}{3}(1+e^{-j\frac{2\pi}{3}}z^{-3}+e^{-j\frac{4\pi}{3}}z^{-6})z^{-k}$. In Fig. 5b, we show the Fourier transform magnitude of the codes. In close accordance with the signature point allocation, the spectra are interleaved and overlapped. We assume the first ($i = 0$) blocks (each of length $K = 2$) sent by the three users are: $\boldsymbol{s}_0(0) = [1, 1]^T$, $\boldsymbol{s}_1(0) = [1, -1]^T$, $\boldsymbol{s}_2(0) = [-1, -1]^T$; and the discrete-time equivalent baseband channels are chosen to be $H_0(z) = 1 + jz^{-1}$, $H_1(z) = 1 + 0.5z^{-1}$, $H_2(z) = 1 + 0.7z^{-1}$, whose nulls are plotted in Fig. 5c. The first noiseless received block can then be computed using (3) as $X(0; z) = 0.33 + (-0.4+0.33j)z^{-1}+(-0.4+0.33j)z^{-2}+(0.33+.58j)z^{-3}+(0.7+0.68j)z^{-4}+(0.2+0.39j)z^{-5}+(0.33-0.58j)z^{-6}+(0.7-0.01j)z^{-7}+(0.2+0.28j)z^{-8}+0z^{-9}+0z^{-10}$, whose magnitude spectrum is depicted in Fig. 5d. The corresponding received spectra of the three respective users are also shown in the same figure with thin lines. We use circles on the composite curve to denote frequencies that correspond to the first user's signature

points and hence they are free of MUI. It can be verified that by applying the $\mathbf{V}_m^{-1}\boldsymbol{G}_m$ operations on $\boldsymbol{x}(i)$ for $m = 0, 1, 2$ respectively, one gets $Y_0(i; z) = 1+(1+j)z^{-1}+jz^{-2}$, $Y_1(i; z) = -1 - 0.5z^{-1} - 0.5z^{-2}$, and $Y_2(i; z) = -1 - 1.7z^{-1} - 0.7z^{-2}$, which are precisely the convolutions of transmitted block symbols with the corresponding channel impulse responses of each user, confirming the equivalent model shown in Fig. 4a. $\square$

V. VANDERMONDE-LAGRANGE AMOUR

In the AMOUR design of Section III, one user's signature points are roots common to all other users [c.f. (6)]. Therefore, whenever one user changes code (to avoid channel nulls for example), or, when a new user enters the cell, all other users in general must change their codes as well in order to maintain transceiver-orthogonality. Our goal in this section is to design the transmit code polynomials $\{C_{m,k}(z)\}_{m=0}^{M-1}$ and the corresponding receive polynomials $\{G_{m,j}(z)\}_{j=0}^{L+K-1}$, $m = 0 \ldots M-1$, so that they possess the same MUI eliminating property as AMOUR, but contrary to AMOUR, only the receiver (base station) needs to change code assignments whenever users change codes, or, whenever new users enter. The dual Vandermonde Lagrange AMOUR system we will develop in this section offers such flexibility in the code assignment procedure and generalizes related results from [17] to the AMOUR framework (see also [31]).

Instead of using Lagrange polynomials $C_{m,k}(z)$ and Vandermonde receive-filters $G_{m,j}(z)$, we will design a dual VL-AMOUR system with Vandermonde transmit- and Lagrange receive- filters. Interchanging roles is also justified from (11) and the commutativity of convolution, which holds since code- and receiver-filters are linear and time-invariant.

Specifically, we adopt code polynomials of order $M(L+K)-1$ with coefficients given by:

$$c_{\mu,k}(p) = A_\mu \sum_{\lambda=0}^{L+K-1} \rho_{\mu,\lambda}^{-P+1+p-k}, \quad p \in [0, P - 1]. \quad (24)$$

Each such code in vector form $\boldsymbol{c}_{\mu,k} := [c_{\mu,k}(0) \ldots c_{\mu,k}(P - 1)]^T$, is a linear combination of $L + K$ Vandermonde vectors: $\boldsymbol{c}_{\mu,k} = A_\mu \sum_{\lambda=0}^{L+K-1} \rho_{\mu,\lambda}^{-P-k+1} \boldsymbol{v}_P(\rho_{\mu,\lambda})$. Note also that the trailing zeros of as1) are not appended in the codes of (24).

We also select Lagrange receive-filters of order $M(L+K)-1$ with transfer functions:

$$G_{m,j}(z) = \prod_{\substack{\mu=0 \\ (\mu,\lambda)\neq(m,j)}}^{M-1} \prod_{\lambda=0}^{L+K-1} \frac{1 - \rho_{\mu,\lambda}z^{-1}}{1 - \rho_{\mu,\lambda}\rho_{m,j}^{-1}}, \quad (25)$$

which can be readily checked to satisfy a condition dual to (3). That is, $\forall\mu \in [0, M - 1]$, $\forall\lambda \in [0, L + K - 1]$,

$$G_{m,j}(\rho_{\mu,\lambda}) = \delta(m - \mu)\delta(j - \lambda). \quad (26)$$

Because filters $\{G_{m,j}(z)\}_{j=0}^{L+K-1}$ are of order $MJ - 1$, the receive-vectors $\boldsymbol{g}_{m,j}^T := [\mathbf{0}_{1\times(L+K-1)}, g_{m,j}(MJ - 1) \cdots g_{m,j}(0)]^T$ are equipped with $P - M(L + K) = L + K - 1$ leading zeros that we denote as $\mathbf{0}_{1\times(L+K-1)}$. These leading receiver-zeros eliminate the part of each received block that is
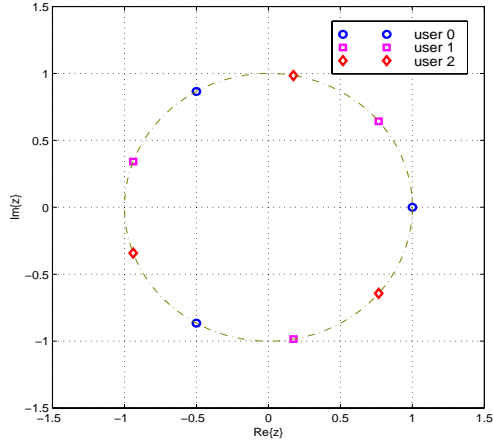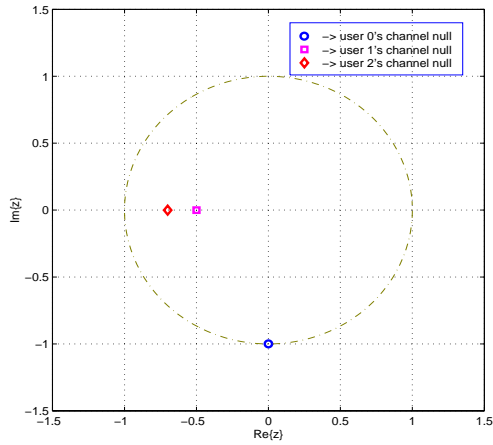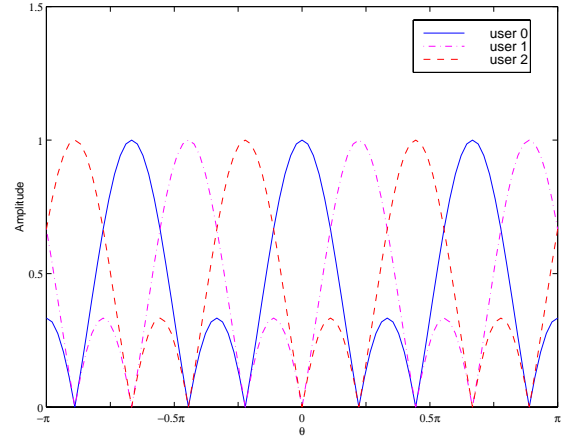
Fig. 5a. The users' signature points

Fig. 5b. The users' transmit-filters in frequency domain
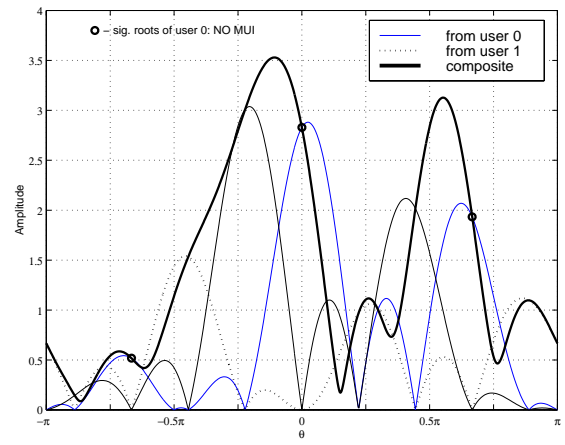

Fig. 5c. Channels' nulls

Fig. 5d. Fourier Transform amplitudes of the received noiseless block

affected by the channel-induced IBI. Their role is analogous to that of discarding the cyclic prefix in an OFDMA receiver.

The Vandermonde codes in (24) do not provide frequency domain user separation as we have achieved in Section III with user-specific (generalized) subcarriers. However, using (26) we will show that the codes in (24) and the receive-filters in (25) satisfy the mutual orthogonality (11); i.e., $\forall l \in [0, L]$ and $\forall m \neq \mu$, $\forall j, k$ it holds that: $[c_{\mu,k}(n - l) \star g_{m,j}(n)]\big|_{n=P-1} = \sum_{p=0}^{P-1} g_{m,j}(p)c_{\mu,k}(P - 1 - p - l) = A_\mu \sum_{\lambda=0}^{L+K-1} \sum_{p=0}^{P-1} g_{m,j}(p)\rho_{\mu,\lambda}^{-p-l-k}$; and hence,

$$[c_{\mu,k}(n - l) \star g_{m,j}(n)]\big|_{n=P-1}$$
$$= A_\mu \sum_{\lambda=0}^{L+K-1} \rho_{\mu,\lambda}^{-l-k} G_{m,j}(\rho_{\mu,\lambda}) = 0 . \quad (27)$$

It can also be verified by direct substitution that the output $Y_m(i; \rho_{m,j}) := \boldsymbol{g}_{m,j}^T \boldsymbol{x}(i)$ of the jth downsampler of the mth user's receiver satisfies [c.f. Fig. 1]

$$Y_m(i; \rho_{m,j}) = A_m S_m(i; \rho_{m,j}) H_m(\rho_{m,j}) + \boldsymbol{g}_{m,j}^T \boldsymbol{\eta}(i). \quad (28)$$

Mimicking the rationale of Section III, the same linear transformations $\mathbf{V}_m^{-1}$ and $\mathbf{\Gamma}_m$ can be applied to $\tilde{\boldsymbol{y}}_m(i) := [Y_m(i; \rho_{m,0})$

$\cdots Y_m(i; \rho_{m,L+K-1})]^T$ successively, in order to recover the symbols $s_m(i; k), \forall k \in [0, K - 1]$.

Therefore, the designed VL-AMOUR transmit- and receive-filters have the same deterministic MUI elimination property as the LV-AMOUR in Section III and also convert the multiuser CDMA system into M parallel single-user systems regardless of the multipath (see Fig. 4a). In addition, since the transmit-filters are linear combinations of the Vandermonde vectors derived from the users' own signature points only, when one user μ changes code (or equivalently signature points), no other user needs to adjust and only the receiver, typically the base station, needs to alter its filters $\{G_{\mu,j}(z)\}_{j=0}^{L+K-1}$ accordingly. This substantially reduces the need for cooperation required among users and thus agrees with the CDMA philosophy.

VI. BLIND EQUALIZATION

Depending on complexity vs. performance tradeoffs, our channel-independent MUI-free receiver can be followed by *any single user equalizer* of linear (e.g., ZF, MMSE) or nonlinear (e.g., DF or ML) form in order to recover the block signal estimates $\hat{\boldsymbol{s}}_m(i)$ from $\boldsymbol{y}_m(i)$. As we mentioned in Section III, AMOUR's built-in ability for channel-independent blind user separation is very attractive even when channels $H_m(z)$ are

available.

However, in order to maintain an overall blind and computationally simple demodulator we can use the single-user blind filterbank approach of [20] that capitalizes on input redundancy which is also present in our transmitter design in the form of L trailing zeros. To show how [20] applies to our single-user setup, let $\boldsymbol{R}_{y_m} := E\{\boldsymbol{y}_m(i)\boldsymbol{y}_m^{\mathcal{H}}(i)\}$ ($^{\mathcal{H}}$ denotes conjugate transpose) be the correlation matrix of $\boldsymbol{y}_m(i) = A_m \mathbf{H}_m \boldsymbol{s}_m(i) + \boldsymbol{\eta}_m(i)$ in (19), which is given by

$$\boldsymbol{R}_{y_m} = A_m^2 \mathbf{H}_m \boldsymbol{R}_{s_m} \mathbf{H}_m^{\mathcal{H}} + \boldsymbol{R}_{\eta_m}, \qquad (29)$$

where $\boldsymbol{R}_{s_m} := E\{\boldsymbol{s}_m(i)\boldsymbol{s}_m^{\mathcal{H}}(i)\}$, and $\boldsymbol{R}_{\eta_m} := E\{\boldsymbol{\eta}_m(i)\boldsymbol{\eta}_m^{\mathcal{H}}(i)\}$ $= E\{\mathbf{V}_m^{-1}\boldsymbol{G}_m\boldsymbol{\eta}(i)\boldsymbol{\eta}^{\mathcal{H}}(i)\boldsymbol{G}_m^{\mathcal{H}}\mathbf{V}_m^{-\mathcal{H}}\} = \mathbf{V}_m^{-1}\boldsymbol{G}_m\boldsymbol{R}_\eta\boldsymbol{G}_m^{\mathcal{H}}\mathbf{V}_m^{-\mathcal{H}}$, with $\boldsymbol{R}_\eta$ denoting the auto-correlation matrix of $\boldsymbol{\eta}(i)$. We assume that $\boldsymbol{R}_{s_m}$ is full rank. Because the Toeplitz matrix $\mathbf{H}_m$ in (20) is also full column rank regardless of the FIR channel, the nullity of $\mathbf{H}_m\boldsymbol{R}_{s_m}\mathbf{H}_m^{\mathcal{H}}$ is L and $\mathrm{Range}(\mathbf{H}_m\boldsymbol{R}_{s_m}\mathbf{H}_m^{\mathcal{H}}) = \mathrm{Range}(\mathbf{H}_m)$. Assuming that $\boldsymbol{R}_\eta$ is known, the noise $\boldsymbol{\eta}_m(i)$ can be whitened by multiplying $\boldsymbol{y}_m(i)$ by any matrix $\boldsymbol{\Phi}_{\eta_m}^{-1}$ such that $\boldsymbol{R}_{\eta_m} = \boldsymbol{\Phi}_{\eta_m}\boldsymbol{\Phi}_{\eta_m}^{-\mathcal{H}}$. The covariance matrix of the prewhitened $\boldsymbol{y}_m$ is

$$\boldsymbol{\Phi}_{\eta_m}^{-1}\boldsymbol{R}_{y_m}\boldsymbol{\Phi}_{\eta_m}^{-\mathcal{H}} = A_m^2\boldsymbol{\Phi}_{\eta_m}^{-1}\mathbf{H}_m\boldsymbol{R}_{s_m}\mathbf{H}_m^{\mathcal{H}}\boldsymbol{\Phi}_{\eta_m}^{-\mathcal{H}} + \boldsymbol{I}. \qquad (30)$$

The signal-plus-noise subspace decomposition of (30) reveals that $\boldsymbol{\Phi}_{\eta_m}^{-\mathcal{H}}\tilde{\boldsymbol{U}}_{y_m}^{(\Phi)}$ is a basis for the null space of $\mathbf{H}_m\boldsymbol{R}_{s_m}\mathbf{H}_m^{\mathcal{H}}$, where $\tilde{\boldsymbol{U}}_{y_m}^{(\Phi)}$ contains the L eigenvectors corresponding to the smallest eigenvalues of $\boldsymbol{\Phi}_{\eta_m}^{-1}\boldsymbol{R}_{y_m}\boldsymbol{\Phi}_{\eta_m}^{-\mathcal{H}}$. Relying on the orthogonality between null and range spaces, it then follows that (see also [20])

$$\tilde{\boldsymbol{U}}_{y_m}^{(\Phi)\mathcal{H}}\boldsymbol{\Phi}_{\eta_m}^{-1}\mathbf{H}_m = \mathbf{0} \;\Rightarrow\; \tilde{\boldsymbol{u}}_l^{\mathcal{H}}\mathbf{H}_m = \mathbf{0}^{\mathcal{H}}, \; l = 1, \ldots, L \quad (31)$$

where $\tilde{\boldsymbol{u}}_l$ denotes the lth column of $\boldsymbol{\Phi}_{\eta_m}^{-\mathcal{H}}\tilde{\boldsymbol{U}}_{y_m}^{(\Phi)}$. Because convolution is commutative, (31) can also be written in terms of the unknown channel coefficients $\boldsymbol{h}_m$ as follows:

$$\tilde{\boldsymbol{u}}_l^{\mathcal{H}}\mathbf{H}_m = \boldsymbol{h}_m^{\mathcal{H}}\boldsymbol{\mathcal{U}} := \boldsymbol{h}_m^{\mathcal{H}}(\boldsymbol{\mathcal{U}}_1 \cdots \boldsymbol{\mathcal{U}}_L) = \mathbf{0}^{\mathcal{H}}, \qquad (32)$$

where each $\boldsymbol{\mathcal{U}}_l$ is an $(L+1) \times K$ Hankel matrix formed by $\tilde{\boldsymbol{u}}_l$ with first column $[\tilde{u}_l(0), \ldots, \tilde{u}_l(L)]^T$ and last row $[\tilde{u}_l(L), \ldots, \tilde{u}_l(L+K-1)]$. From (32), the channel vector $\boldsymbol{h}_m$ can be obtained as the *unique* (within a scale factor) null eigenvector of $\boldsymbol{\mathcal{U}}$ [20].

In practice, the method is implemented by replacing the ensemble covariance matrices by sample averages. When the latter are formed by averaging more than K blocks $\boldsymbol{y}_m(i)$, the sample estimate of $\boldsymbol{R}_{s_m}$ will be full rank almost surely. In short, the mth receiver collects $I \geq K$ blocks of $\boldsymbol{y}_m(i)$ in an $(L+K) \times I$ matrix $\boldsymbol{Y}_m := [\boldsymbol{y}_m(0) \cdots \boldsymbol{y}_m(I-1)]$ and forms

$$\frac{1}{I}\boldsymbol{Y}_m\boldsymbol{Y}_m^{\mathcal{H}} = \frac{1}{I}(A_m^2\mathbf{H}_m\boldsymbol{S}_m\boldsymbol{S}_m^{\mathcal{H}}\mathbf{H}_m^{\mathcal{H}} + \mathbf{V}_m\mathbf{V}_m^{\mathcal{H}})$$

$$= \frac{1}{I}(A_m^2\mathbf{H}_m\boldsymbol{S}_m\boldsymbol{S}_m^{\mathcal{H}}\mathbf{H}_m^{\mathcal{H}} + \mathbf{V}_m\boldsymbol{G}_m\mathbf{V}\mathbf{V}^{\mathcal{H}}\boldsymbol{G}_m^{\mathcal{H}}\mathbf{V}_m^{\mathcal{H}}), \quad (33)$$

where $\boldsymbol{S}_m := [\boldsymbol{s}_m(0) \cdots \boldsymbol{s}_m(I-1)]_{K \times I}$, $\mathbf{V}_m := [\boldsymbol{\eta}_m(0) \cdots \boldsymbol{\eta}_m(I-1)]_{P \times I}$, and $\mathbf{V} := [\boldsymbol{\eta}(0) \cdots \boldsymbol{\eta}(I-1)]_{P \times I}$. The sample averages in (33) will converge in the mean square sense to the ensemble covariance matrices (note that $\boldsymbol{y}_m(i)$ in (19) is mixing because $s_m(n)$ has finite moments and $h_m(n)$ is FIR). Finally, because $\boldsymbol{\Phi}_{\eta_m}^{-\mathcal{H}}\tilde{\boldsymbol{U}}_{y_m}^{(\Phi)}$ is a continuous function of $\boldsymbol{R}_{y_m}$ and the estimate $\hat{\boldsymbol{R}}_{y_m} = I^{-1}\boldsymbol{Y}_m\boldsymbol{Y}_m^{\mathcal{H}}$ is consistent, it follows that the channel estimators are also consistent.

Once $\mathbf{H}_m$ is found, a zero forcing equalizer $\boldsymbol{\Gamma}_m^{(zf)} = \mathbf{H}_m^\dagger$, or, an MMSE (Wiener) equalizer

$$\boldsymbol{\Gamma}_m^{(mmse)} = A_m\boldsymbol{R}_{s_m}\mathbf{H}_m^{\mathcal{H}}(\boldsymbol{R}_{\eta_m} + A_m^2\mathbf{H}_m\boldsymbol{R}_{s_m}\mathbf{H}_m^{\mathcal{H}})^{-1}, \quad (34)$$

can be applied to the vector $\boldsymbol{y}_m(i)$ to obtain estimates of the symbols $\boldsymbol{s}_m(i)$. Direct and adaptive equalizers are also possible (see e.g., [20] for details). Derivation of the equalizer, its adaptive implementation, and its performance analysis will not be pursued in this paper. However, we want to underscore that unlike AMOUR, all existing blind CDMA schemes [1, 5, 12, 23, 24, 26] do not guarantee channel-independent identifiability in the uplink; e.g., reducible transfer function matrices offer counterexamples as recognized by [23]. Some also rely on whiteness assumptions which may fail for coded inputs and require additional (e.g., antenna) diversity to ameliorate (but not eliminate) channel fades [5].

VII. PERFORMANCE AND COMPARISONS

Because $\eta(n)$ in (2) is AGN, theoretical BER evaluation is possible for a given constellation when we adopt a ZF equalizer $\boldsymbol{\Gamma}_m^{(zf)}$. For simplicity, we focus first on BPSK $s_m(n)$'s and the downlink setup (same $H_m(z) = H(z), \forall m$). The mth user's ZF receiver can be described by the matrix: $\bar{\boldsymbol{G}}_m := \mathbf{H}_m^\dagger\mathbf{V}_m^{-1}\boldsymbol{G}_m$, whose kth row is denoted as $\bar{\boldsymbol{g}}_{mk}^{\mathcal{H}}$. Our figure of merit is the average BER

$$\bar{P}_e := (MK)^{-1}\sum_{m=0}^{M-1}\sum_{k=0}^{K-1}P_{e,mk}, \qquad (35)$$

where $P_{e,mk}$ denotes BER for the kth symbol of user m. Because

$$\hat{s}_m(iK+k) = A_m s_m(iK+k) + \bar{\boldsymbol{g}}_{mk}^{\mathcal{H}}\boldsymbol{\eta}(i), \qquad (36)$$

our SNR will be $A_m^2/(N_0\bar{\boldsymbol{g}}_{mk}^{\mathcal{H}}\bar{\boldsymbol{g}}_{mk}/2)$ and with $2E_b/N_0$ denoting bit SNR, we have $A_m^2 = E_b/E_{c,m}$ where $E_{c,m} := \sum_{p=0}^{M(L+K)-1}|c_m(p)|^2$ is the energy of the mth user's code (note that $E_{c,m}$ is the same $\forall m$ when the $\rho_{m,j}$'s chosen as in (22)); hence,

$$P_{e,mk} = \mathcal{Q}\left(\sqrt{\frac{1}{\bar{\boldsymbol{g}}_{mk}^{\mathcal{H}}\bar{\boldsymbol{g}}_{mk}E_{c,m}}}\sqrt{\frac{2E_b}{N_0}}\right), \qquad (37)$$

where $\mathcal{Q}(\cdot)$ denotes the $\mathcal{Q}$-function.

In comparison, M-user OFDMA will exhibit at the mth equalizer's output

$$SNR_m = |H(e^{j\frac{2\pi m}{M}})|^2 E_b/(N_0/2), \qquad (38)$$

and thus average BER:

$$\bar{P}_e = \frac{1}{M}\sum_{m=0}^{M-1}\mathcal{Q}\left(|H(e^{j\frac{2\pi m}{M}})|\sqrt{\frac{2E_b}{N_0}}\right), \qquad (39)$$
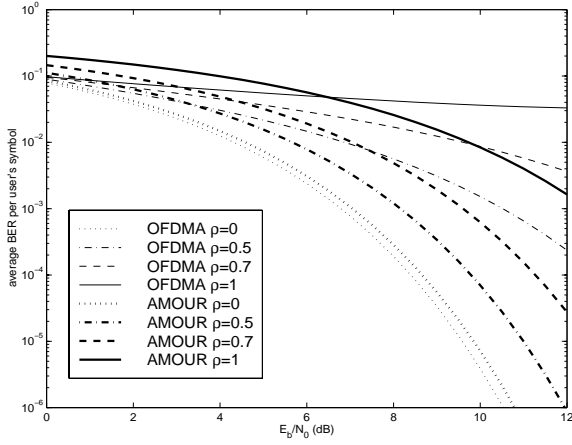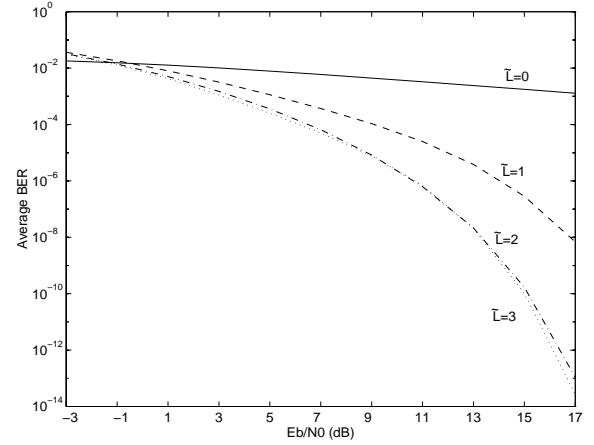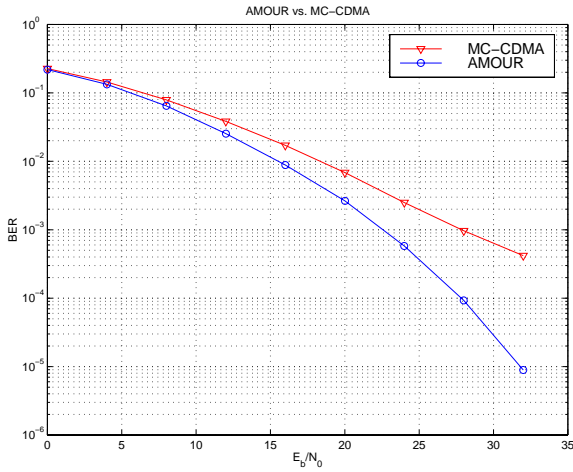
Fig. 6a. AMOUR vs. OFDMA, 16 users, $L = 1$

Fig. 6b. AMOUR with $\tilde{L} < L = 6$ (Rayleigh fading)

Fig. 7. Comparing AMOUR with MC-CDMA MMSE receivers

where $H(z)$ is for OFDMA, a channel common to all users (downlink setup).

Test case 1: We compared (35) with (39) on a system with $M = 16$ users sharing a common multipath channel of order $L = 1$ having a single root located at $\rho = 0, 0.5, 0.7, 1$. Because OFDMA's spreading gain is $(M + L)/M$, for a fair comparison with AMOUR, we chose $K = M = 16$ [c.f. (15)]. Fig. 6a shows BER gains of ZF AMOUR over OFDMA by 2-3 orders of magnitude as the fading becomes more severe (ρ approaches the unit circle).

Test case 2: To avoid channel dependent performance bias, we averaged (35) over 100 Monte Carlo realizations of 6th order Rayleigh faded channels (simulated with complex Gaussian coefficients) and obtained AMOUR's $\bar{P}_e$ vs E_b/N_0 curves parameterized by the number of signature points $\tilde{L}$ assigned to each of the $M = 16$ users (see Fig. 6b). Values of K were chosen according to (15) to maintain the same rate. Notwithstanding, even small values of the diversity factor $\tilde{L}$ offer considerable BER gains over OFDMA ($\tilde{L} = 0$).

Test case 3: We compared the performance of AMOUR with codes as in (23) and $M = 16$, $L = 2$, $K = 8$, against an MC-CDMA system with Walsh-Hadamard spreading codes im-

plemented as in e.g., [8, Figure 3]. At the MC-CDMA transmitter, every user serial-to-parallel converts the input bit stream to K low rate substreams, each of which is spread in the frequency domain by the same user-dependent Walsh-Hadamard code of length 16. The frequency domain spreading is implemented using time-domain spreading followed by OFDM. The subcarriers used by different substreams do not overlap. At the receiver end, both systems use MMSE equalization and both assume perfect knowledge of the channels. Fig. 7 shows the corresponding BERs averaged over 45 independent Rayleigh fading channels. AMOUR clearly outperforms MC-CDMA especially at high SNR, indicating the importance of AMOUR's ability to eliminate MUI and ISI which are the major causes of performance degradation in multiple access systems.

Test case 4: To test AMOUR's ability for channel independent blind demodulation in uplink systems, we simulated $M = 4$ users each transmitting blocks of $K = 16$ QPSK symbols with $L + K = 17$ signature points, through a two-ray channel ($L = 1$). The signature points were equally spaced and interleaved along the unit circle as in (22). Relying only on $I = L + K = 34$ blocks received in AWGN ($E_s/N_0 = 15$dB), we recovered each user's constellation using the FIR-ZF blind equalizer described in Section VI. The received data and the equalized scatter diagram for one user's data are depicted in Figs. 8a and 8b, respectively. Decision feedback (DF) schemes (see e.g., [28]) can improve performance further. We stress however, that our basic result does not rely on finite alphabet assumptions; thus, it applies to general deterministic blind separation and equalization of convolutive mixtures involving even continuous amplitude precoded (e.g., radar or speech) sources.

Test case 5: To quantify AMOUR's performance for blind equalization in uplink CDMA systems, we used the blind method outlined in Section VI, which first estimates the channels and then applies zero-forcing or MMSE equalization. We simulated 100 Monte-Carlo realizations of Rayleigh channels of order 1, and tested performance when $I = 34$ or $I = 100$ blocks were received. It follows from (33) that the minimum number of blocks required in order to implement the method is $I = L + K = 17$ [20]. Blind performance is shown against the theoretical one computed using formula (35) with perfect channel information (see Figs. 8c and 8d). We observe that with
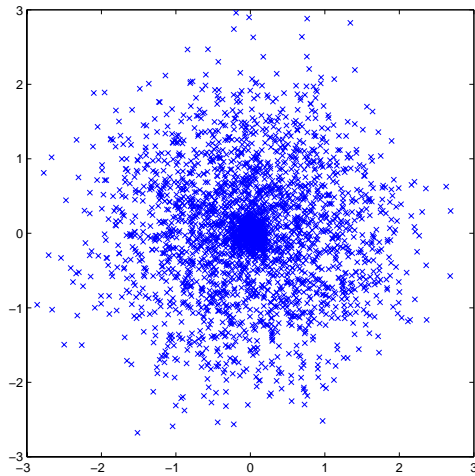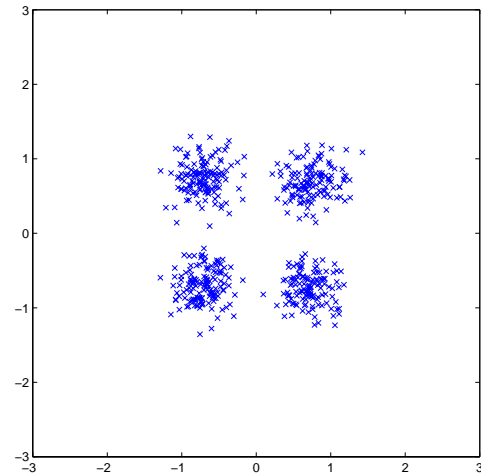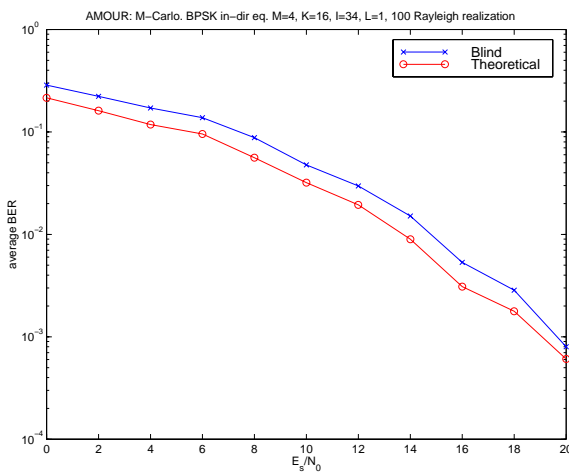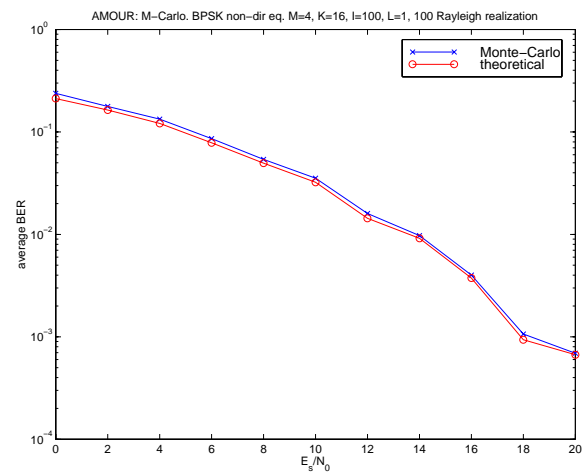
Fig. 8a. Received signal ($E_s/N_0 = 15dB$).

Fig. 8b. Blindly equalized constellation of one user

Fig. 8c. $I = 34$

Fig. 8d. $I = 100$

$I = 34$ blocks (Fig. 8c) the blind method undergoes only a small (2dB) penalty compared with the theoretical bound (35), and as I increases to 100, the blind method can virtually achieve the known-channel bound for all simulated $SNRs$ (> 0). The latter supports substantially the blind equalization of users' symbols as promised by our system design and speaks for AMOUR's potential in a wireless multipath environment.

VIII. CONCLUSIONS

We developed a flexible so-termed AMOUR system especially suitable for blind uplink CDMA. Relying on block-symbol spreading, the system was shown to be capable of eliminating MUI deterministically and assuring identifiability of input symbols in the presence of frequency-selective multipath without resorting to multiple channel diversity (only an upper bound on the channel order was assumed available). Blind equalizers within the AMOUR framework were derived and performance of zero-forcing and MMSE solutions was analyzed and compared with OFDMA and MC-CDMA for fixed and slow Rayleigh fading channels. Tests and numerical simulations demonstrated the system's generality, flexibility, superior performance, and strong potential in multiuser communications.

For recent results on related subjects the reader is referred to [6, 13, 22, 33] (see also [31, 32] for tutorial treatments).

REFERENCES

[1] S. E. Bensley and B. Aazhang, "Subspace-based channel estimation for code division multiple access communication systems," *IEEE Transactions on Communications*, vol. 44, pp. 1009–1020, Aug. 1996.

[2] Q. Chen, E. S. Sousa, and S. Pasupathy, "Multicarrier CDMA with adaptive frequency-hopping for mobile radio systems," *IEEE Journal on Selected Areas in Communications*, pp. 1852–1857, Dec. 1996.

[3] V. M. DaSilva and E. S. Sousa, "Multicarrier orthogonal CDMA signals for quasi-synchronous communication systems," *IEEE Journal on Selected Areas in Communications*, pp. 842–852, June 1994.

[4] K. Fazel and G. P. Fettweis (Eds), *Multi-Carrier Spread Spectrum*, Kluwer Academic Publishers, 1997.

[5] D. Gesbert, J. Sorelius, and A. Paulraj, "Blind multi-user MMSE detection of CDMA signals," in *Proc. of Intl. Conf. on ASSP*, May 1998, pp. 3161–3164.

[6] G. B. Giannakis, P. A. Anghel, and Z. Wang, "All-digital unification and equalization of generalized multi-carrier CDMA through frequency-selective uplink channels," *IEEE Transactions on Communications*, Apr. 2000 (submitted); see also *Prof. of ICASSP*, Istanbul, Turkey,June5–9, 2000.

[7] X. Gui and T. S. Ng, "Performance of Asynchronous Orthogonal Multicarrier CDMA system in Frequency Selective Fading Channel," *IEEE Transactions on Communications*, pp. 1–84–1091, July 1999.

[8] S. Hara and R. Prasad, "Overview of multicarrier CDMA," *IEEE Communications Magazine*, pp. 126–133, Dec. 1997.

[9]   R. A. Iltis, "Performance of constrained and unconstrained adaptive multiuser detectors for quasi-synchronous CDMA," *IEEE Transactions on Communications*, vol. 46, no. 1, pp. 135–431, Jan. 1998.

[10] S. Kaiser and K. Fazel, "A spread spectrum multi-carrier multiple access system for mobile communications," in *MCSS*, Oberpfaffenhofen, Germany, 1997, pp. 49–56, Kluwer Academic Publishers [4].

[11] S. Kondo and L. B. Milstein, "Performance of multicarrier DS CDMA systems," *IEEE Transactions on Communications*, vol. 44, no. 2, pp. 238–46, Feb. 1996.

[12] H. Liu and G. Xu, "A subspace method for signature waveform estimation in synchronous CDMA systems," *IEEE Transactions on Communications*, vol. 44, no. 10, pp. 1346–1354, Oct. 1996.

[13] Z. Liu and G. B. Giannakis, "Space-time coding with transmit antennas for multiple access regardless of frequency-selective multipath," in *Proc. of the 1st Sensor Array and Multichannel SP Workshop*, Boston, MA, Mar. 15-17, 2000.

[14] E. Nikula, A. Toskala, E. Dahlman, L. Girard, and A. Klein, "FRAMES multiple access for UMTS and IMT-2000," *IEEE Personal Communications*, pp. 16–24, April 1998.

[15] D. N. Rowitch and L. B. Milstein, "Convolutionally coded multicarrier DS-CDMA systems in a multipath fading channel — Part I: Performance analysis," *IEEE Transactions on Communications*, vol. 47, no. 10, pp. 1570–1582, Oct. 1999.

[16] H. Sari, "Orthogonal frequency-division multiple access with frequency hopping and diversity," in *MCSS*. 1997, pp. 57–68, Kluwer Academic Publishers [4].

[17] A. Scaglione, S. Barbarossa, and G. B. Giannakis, "Fading-resistant and MUI-free codes for CDMA systems," in *Proc. of Intl. Conf. on ASSP*, Phoenix, AZ, Mar. 1999.

[18] A. Scaglione and G. B. Giannakis, "Design of user codes in QS-CDMA systems for MUI elimination in unknown multipath," *IEEE Communications Letters*, pp. 25–27, Feb. 1999.

[19] A. Scaglione, G. B. Giannakis, and S. Barbarossa, "Redundant filterbank precoders and equalizers Part I: Unification and optimal designs," *IEEE Transactions on Signal Processing*, vol. 47, pp. 1988–2006, July 1999.

[20] A. Scaglione, G. B. Giannakis, and S. Barbarossa, "Redundant filterbank precoders and equalizers Part II: Blind channel estimation, synchronization, and direct equalization," *IEEE Transactions on Signal Processing*, vol. 47, pp. 2007–2022, July 1999.

[21] E. Sourour and M. Nakagawa, "Performance of orthogonal multicarrier CDMA in a multipath fading channel," *IEEE Transactions on Communications*, vol. 44, no. 3, pp. 356–67, Mar. 1996.

[22] A. Stamoulis and G. B. Giannakis, "Packet fair queueing scheduling based on multirate multipath-transparent CDMA for wireless networks," *IEEE Transactions on Communications*, Aug. 1999 (submitted); see also *Proc. of INFOCOM*, Tel-Aviv, Israel, Mar. 26–30, 2000.

[23] M. K. Tsatsanis, "Inverse filtering criteria for CDMA systems," *IEEE Transactions on Signal Processing*, vol. 45, no. 1, pp. 102–112, Jan. 1997.

[24] M. K. Tsatsanis and G. B. Giannakis, "Multirate filter banks for code-division multiple access systems," in *Proc. of Intl. Conf. on ASSP*, New York, NY, USA, 1995, vol. 2, pp. 1484–7.

[25] M. K. Tsatsanis and G. B. Giannakis, "Optimal decorrelating receivers for DS-CDMA systems: A signal processing framework," *IEEE Transactions on Signal Processing*, vol. 44, no. 12, pp. 3044–55, Dec. 1996.

[26] M. K. Tsatsanis and Z. Xu, "Performance analysis of minimum variance CDMA receiver," *IEEE Transactions on Signal Processing*, vol. 46, no. 11, pp. 3014–22, Nov. 1998.

[27] L. Vandendorpe, L. Cuvelier, and O. van de Wiel, "Fractionally spaced linear and decision-feedback detectors for transmultiplexers," *IEEE Transactions on Signal Processing*, vol. 46, no. 4, pp. 996–1011, Apr. 1998.

[28] S. Verdú, *Multiuser Detection*, Cambridge Press, 1998.

[29] B. R. Vojčić and W. M. Jang, "Transmitter precoding in synchronous multiuser communications," *IEEE Transactions on Communications*, vol. 46, no. 10, pp. 1346–1355, Oct. 1998.

[30] X. Wang and H. V. Poor, "Iterative (Turbo) soft interference cancellation and decoding for coded CDMA," *IEEE Transactions on Communications*, vol. 46, no. 7, pp. 1046–1061, July 1999.

[31] Z. Wang and G. B. Giannakis, "Block spreading for multipath-resilient generalized multi-carrier CDMA," in *Signal Processing Advances in Wireless Communications*, G. B. Giannakis, Y. Hua, P. Stoica, and L. Tong, Eds. 2000 (to appear), vol. II, Chapter 9, Prentice-Hall, Inc.

[32] Z. Wang and G. B. Giannakis, "Wireless multicarrier communications: where Fourier meets Shannon," *IEEE Signal Processing Magazine*, May 2000.

[33] Z. Wang and G. B. Giannakis, "Block Spreading for MUI/ISI-Resilient Generalized Multi-carrier CDMA with Multirate Capabilities," in *Proc. of Intl. Conf. on Communications*, New Orleans, LA, June 18–22, 2000.